

---

This is an electronic reprint of the original article.

This reprint may differ from the original in pagination and typographic detail.

Author(s): Tynell, Tommi & Yamauchi, Hisao & Karppinen, Maarit

Title: Hybrid inorganic organic superlattice structures with atomic layer deposition/molecular layer deposition

Year: 2014

Version: Final published version

**Please cite the original version:**

Tynell, Tommi & Yamauchi, Hisao & Karppinen, Maarit. 2014. Hybrid inorganic organic superlattice structures with atomic layer deposition/molecular layer deposition. Journal of Vacuum Science & Technology A: Vacuum, Surfaces, and Films. Volume 32, Issue 1. 01A105/1-5. ISSN 0734-2101 (printed). DOI: 10.1116/1.4831751.

Rights: © 2014 American Vacuum Society. This article may be downloaded for personal use only. Any other use requires prior permission of the authors and the American Institute of Physics. The following article appeared in Journal of Vacuum Science & Technology A: Vacuum, Surfaces, and Films. Volume 32, Issue 1 and may be found at <http://scitation.aip.org/content/avs/journal/jvsta/32/1/10.1116/1.4831751>.

---

All material supplied via Aaltodoc is protected by copyright and other intellectual property rights, and duplication or sale of all or part of any of the repository collections is not permitted, except that material may be duplicated by you for your research use or educational purposes in electronic or print form. You must obtain permission for any other use. Electronic or print copies may not be offered, whether for sale or otherwise to anyone who is not an authorised user.

## Hybrid inorganic–organic superlattice structures with atomic layer deposition/molecular layer deposition

Tommi Tynell, Hisao Yamauchi, and Maarit Karppinen

Citation: *Journal of Vacuum Science & Technology A* **32**, 01A105 (2014); doi: 10.1116/1.4831751

View online: <http://dx.doi.org/10.1116/1.4831751>

View Table of Contents: <http://scitation.aip.org/content/avs/journal/jvsta/32/1?ver=pdfcov>

Published by the AVS: Science & Technology of Materials, Interfaces, and Processing

### Articles you may be interested in

[On the environmental stability of ZnO thin films by spatial atomic layer deposition](#)

*J. Vac. Sci. Technol. A* **31**, 061504 (2013); 10.1116/1.4816354

[Effect of disorder on carrier transport in ZnO thin films grown by atomic layer deposition at different temperatures](#)

*J. Appl. Phys.* **114**, 043703 (2013); 10.1063/1.4815941

[Effect of in situ hydrogen plasma treatment on zinc oxide grown using low temperature atomic layer deposition](#)


*J. Vac. Sci. Technol. A* **31**, 01A124 (2013); 10.1116/1.4767813

[Atomic layer deposition of Al-doped ZnO thin films](#)




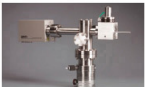
*J. Vac. Sci. Technol. A* **31**, 01A109 (2013); 10.1116/1.4757764

[Structural, electrical, and optical properties of atomic layer deposition Al-doped ZnO films](#)

*J. Appl. Phys.* **108**, 043504 (2010); 10.1063/1.3466987



## Instruments for Advanced Science

<p>Contact Hiden Analytical for further details:  <b>W</b> <a href="http://www.HidenAnalytical.com">www.HidenAnalytical.com</a>  <b>E</b> <a href="mailto:info@hiden.co.uk">info@hiden.co.uk</a>  <a href="#">CLICK TO VIEW</a> our product catalogue</p>	 <p><b>Gas Analysis</b></p> <ul style="list-style-type: none"> <li>› dynamic measurement of reaction gas streams</li> <li>› catalysis and thermal analysis</li> <li>› molecular beam studies</li> <li>› dissolved species probes</li> <li>› fermentation, environmental and ecological studies</li> </ul>	 <p><b>Surface Science</b></p> <ul style="list-style-type: none"> <li>› UHV-TPD</li> <li>› SIMS</li> <li>› end point detection in ion beam etch</li> <li>› elemental imaging - surface mapping</li> </ul>	 <p><b>Plasma Diagnostics</b></p> <ul style="list-style-type: none"> <li>› plasma source characterization</li> <li>› etch and deposition process reaction</li> <li>› kinetic studies</li> <li>› analysis of neutral and radical species</li> </ul>	 <p><b>Vacuum Analysis</b></p> <ul style="list-style-type: none"> <li>› partial pressure measurement and control of process gases</li> <li>› reactive sputter process control</li> <li>› vacuum diagnostics</li> <li>› vacuum coating process monitoring</li> </ul>
---	--	--	--	--

# Hybrid inorganic–organic superlattice structures with atomic layer deposition/molecular layer deposition

Tommi Tynell, Hisao Yamauchi, and Maarit Karppinen<sup>a)</sup>

*Department of Chemistry, Aalto University, FI-00076 Aalto, Finland*

(Received 23 August 2013; accepted 4 November 2013; published 15 November 2013)

A combination of the atomic layer deposition (ALD) and molecular layer deposition (MLD) techniques is successfully employed to fabricate thin films incorporating superlattice structures that consist of single layers of organic molecules between thicker layers of ZnO. Diethyl zinc and water are used as precursors for the deposition of ZnO by ALD, while three different organic precursors are investigated for the MLD part: hydroquinone, 4-aminophenol and 4,4'-oxydianiline. The successful superlattice formation with all the organic precursors is verified through x-ray reflectivity studies. The effects of the interspersed organic layers/superlattice structure on the electrical and thermoelectric properties of ZnO are investigated through resistivity and Seebeck coefficient measurements at room temperature. The results suggest an increase in carrier concentration for small concentrations of organic layers, while higher concentrations seem to lead to rather large reductions in carrier concentration. © 2014 American Vacuum Society.

[<http://dx.doi.org/10.1116/1.4831751>]

## I. INTRODUCTION

Hybrid materials combining inorganic and organic constituents attract rapidly growing interest due to their potential in creating materials with novel combinations of material properties. Relatively simple inorganic–organic composite materials<sup>1,2</sup> may be used to create complex hybrid frameworks including superlattices and nanolaminates of alternating inorganic and organic layers.<sup>3–5</sup> Flexible conductors, solar cells, and gas-permeation barrier layers are some of the applications proposed for these nanostructured hybrid materials, and the practically endless variety of organic molecules available should lead to other novel applications as the field develops further.

Atomic layer deposition (ALD) exhibits many features such as excellent process controllability and conformality of the resultant thin films and coatings that, combined with its counterpart for organic materials, molecular layer deposition (MLD), makes it an ideal technique for the fabrication of hybrid thin-film structures. There are a growing number of reports on various hybrid thin films fabricated with ALD/MLD,<sup>6–16</sup> but the focus has primarily been on homogeneous 1:1 inorganic–organic hybrid materials where single layers of the organic constituent alternate with single layers of the inorganic part, and then also on so-called nanolaminate structures built up of considerably thicker layers of the two constituents. Despite the potential usefulness of superlattices consisting of very thin layers of one material between thicker layers of another, there are very few reports of the fabrication of hybrid superlattices using ALD/MLD.<sup>7,17</sup>

Zinc oxide is a semiconductor with a wide variety of potential applications from optoelectronics to thin-film transistors, and consequently it has been the subject of a concentrated research effort using all the major thin-film deposition technologies, including ALD.<sup>18,19</sup> The applicability of ZnO

is largely based on its useful combination of transparency to visible light and controllable carrier concentration, so the challenge in ZnO thin-film fabrication has typically been the creation of high-quality films with the desired carrier concentration. Incorporation of organic layers into ZnO was recently shown to have an effect on its electrical properties, but the effect has not been thoroughly studied as of yet.<sup>20</sup> Besides its optoelectronic properties, ZnO is also a promising thermoelectric oxide material. Nevertheless, the influence of organic layers on ZnO's thermoelectric properties has not been widely studied either. The fabrication of a hybrid superlattice structure would be especially interesting, considering that superlattices are expected to have potentially large effects on materials' thermoelectric performance due to effects from phonon inhibition and charge confinement.<sup>21–23</sup>

In this work, we demonstrate that the ALD/MLD method can be used to fabricate hybrid inorganic–organic superlattice structures consisting of a thicker ZnO layer and single layers of appropriate organic molecules; here this is shown for hydroquinone, 1,4-aminophenol, and oxydianiline molecules. All the three different organic layers have a similar, slightly nonlinear effect on the electrical and thermoelectric properties of the ZnO films.

## II. EXPERIMENT

### A. Thin film depositions

Zinc oxide films interspersed with layers of organic molecules were grown on borosilicate glass and silicon substrates using an F-120 ALD reactor from ASM Microchemistry. The ZnO to organic layer ratio was varied between 199:1 and 39:1, and the organic layers were deposited in a periodically repeating way in order to create a superlattice structure. The precursors for the ZnO layers were diethyl zinc (DEZ) and water, while hydroquinone (HQ), 4-aminophenol (AP), or 4,4'-oxydianiline (ODA) was used for the deposition of organic layers. The deposition temperature for all the

<sup>a)</sup>Electronic mail: [maarit.karppinen@aalto.fi](mailto:maarit.karppinen@aalto.fi)

depositions was 220 °C, the DEZ and water were unheated, and precursor temperatures of 120, 111, and 153 °C, respectively, were used for HQ, AP, and ODA. The deposition process consisted of a total of 600 cycles, with pulsing/purging times of 1.0/1.5 s for DEZ, 1.5/2.0 s for water, 8.0/12.0 s for HQ and AP, and 14.0/14.0 s for ODA.

## B. Sample characterization

X-ray reflectivity (XRR) measurements were carried out to determine the thickness of the films as well as establish the presence of superlattice structures. Grazing-incidence x-ray diffraction (GIXRD) was employed to observe possible changes in the crystallinity and/or crystal structure of the films. Both measurements were performed using a PANalytical X'Pert Pro x-ray diffractometer with a Cu K $\alpha$  x-ray source.

Fourier transform infrared (FTIR) spectroscopy was used to determine the character of the bonds in the hybrid thin films and ascertain the type of organic constituent present in the films. For this purpose, films with exceptionally large numbers of organic layers (ratio of 3:1) were deposited on Si substrates.

Seebeck coefficient and resistivity values were measured for the hybrid films grown on borosilicate glass at room temperature using a homemade measurement setup. The resistivity measurement consisted of a simple four-point measurement probe, while the determination of the Seebeck coefficient was carried out by affixing the sample between two Cu plates with silver paste and applying a temperature gradient over it.

## III. RESULTS AND DISCUSSION

### A. Growth characteristics

The combined ALD/MLD depositions produced thin films of excellent uniformity with thicknesses mostly in the 90–100 nm range, as determined with XRR analysis. The XRR measurements also revealed clear signs of superlattice structures in all the hybrid films as can be seen in Figs. 1 and 2, in

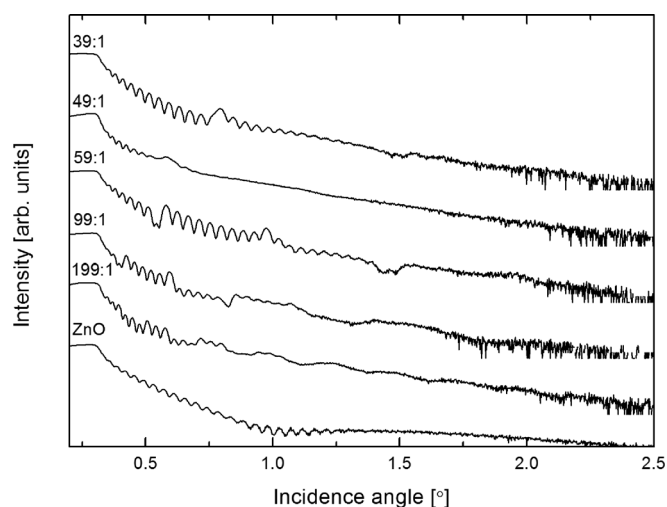


FIG. 1. XRR patterns for the ZnO:AP thin films. The vertical axis is presented in logarithmic scale.

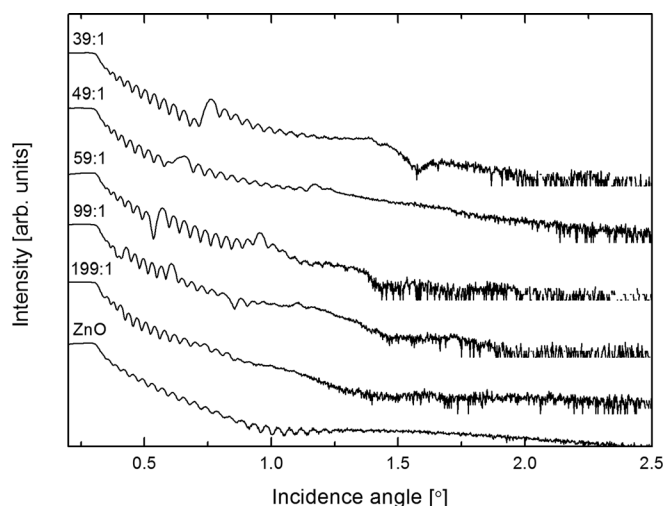


FIG. 2. XRR patterns for the ZnO:ODA films. The vertical axis is presented in logarithmic scale.

which the XRR patterns for the ZnO:AP and ZnO:ODA films are displayed. The interference of the reflections from the different layers of a superlattice structure causes the formation of a characteristic group of peaks within the XRR pattern, the shape of which is directly related to the number of superlattice repetitions present in the film. Ideally, a group of peaks consisting of  $N - 2$  smaller peaks flanked by two larger superlattice peaks will be observed in the XRR pattern, where  $N$  is the number of superlattice repetitions, i.e., in this case, the number of organic layers in the film. The superlattice peak shapes in Figs. 1 and 2 exactly match the intended number of organic layers in the films for ratios of 99:1 and 59:1 (and for ZnO:ODA, also 49:1), confirming the incorporation of organic layers into the film as well as the formation of the intended superlattice structure. For the films with other ZnO:organic layer ratios, the exact number of superlattice repetitions cannot be determined due to the lack of peak resolution, but the patterns still clearly display the type of shape identifying the presence of a superlattice in the structure. GIXRD measurements showed no changes in the positions of the ZnO diffraction peaks or the degree of crystallinity of the sample, indicating that the organic layers have little effect on the ZnO structure as a whole.

The XRR patterns for the ZnO:organic hybrid films were simulated using the X'Pert Reflectivity program; the final fitting parameters are collected in Table I (rows with missing values could not be properly fitted). The fitting was done so that the ZnO layers between organic layers (within the superlattice) were distinguished from the layers between the substrate and the first organic layer as well as the final ZnO layer on top of the last organic layer. Disregarding some outliers, it is possible to see several trends in the parameters in Table I. First of all, the organic layers seem to have little to no hindering effect on the growth of the subsequent ZnO layers judging by the growth rate of ZnO between the organic layers: 1.62–1.76 Å/cycle for ZnO:HQ, 1.44–1.69 Å/cycle for ZnO:AP, and 1.51–1.61 Å/cycle for ZnO:ODA. All these values are quite normal for ZnO at 220 °C and essentially unchanged from the 1.65 Å/cycle value that was determined



TABLE I. Fitting parameters for fitting of the XRR patterns of the ZnO: organic thin films. The  $t_1$ ,  $t_2$ , and  $t_3$  values in the ZnO column correspond to the thicknesses of the “blocks” of ZnO between the substrate and the first organic layer ( $t_1$ ), between two organic layers in the superlattice ( $t_2$ ), and on top of the last organic layer ( $t_3$ ).  $\rho$  in this table stands for density.

	ZnO					Organic		
	$t_1$ (nm)	$t_2$ (nm)	$t_3$ (nm)	$\rho$ (g/cm <sup>3</sup> )	Roughness (nm)	$t$ (nm)	$\rho$ (g/cm <sup>3</sup> )	Roughness (nm)
<b>ZnO:HQ</b>								
199:1	9	34.7	15.6	5.0	1.5	0.55	3.3	0.57
99:1	6.9	16.8	6.5	5.25	1.4	0.51	2.3	1.1
74:1	5.0	12.0	6.7	5.27	1.35	0.33	2.2	0.8
59:1	4.0	9.7	2.6	5.2	1.1	0.55	1.8	1.2
49:1	1.7	8.6	1.5	5.25	1.0	0.55	2.8	1.4
<b>ZnO:AP</b>								
199:1	—	—	—	—	—	—	—	—
99:1	9.8	16.7	8.3	5.3	1.1	0.52	3.7	1.2
74:1	2.5	12.1	3.9	5.28	1.2	0.45	3.4	1.7
59:1	4.3	8.5	5.1	5.3	1.15	0.6	3.9	1.35
49:1	—	—	—	—	—	—	—	—
<b>ZnO:ODA</b>								
199:1	—	—	—	—	—	—	—	—
99:1	3.7	15.7	7.9	5.2	1.3	0.6	3.8	1.4
74:1	6.3	11.3	6.3	5.2	1.3	0.42	3.8	1.6
59:1	4.7	9.5	4.9	4.1	0.7	0.8	3.7	0.8
49:1	2.2	7.4	3.3	5.2	1.4	0.74	3.9	0.7

for pure ZnO in this study. There is, however, a constantly lower  $t_2$  value obtained for ZnO:ODA compared to ZnO:HQ, suggesting that there is indeed a small nucleation delay or other hindering effect on ZnO growth following the organic layers of ODA. The density of the ZnO layers falls within 5.2–5.3 g/cm<sup>3</sup> for most of the films, which is reasonably close to the theoretical value of 5.61 g/cm<sup>3</sup>. There also appears to be a decreasing trend in the roughness of ZnO with increasing HQ content, but more data would be necessary to draw reliable conclusions from this, especially as there does not seem to be much of a change observed with AP or ODA.

The fitted parameters for the MLD layers in the superlattice structure are included in Table I as well, although care should be taken when considering them due to the added uncertainty in simulating a single layer of material. Nonetheless, several trends can be observed here as well, starting with the thickness of the layers, which mostly fall within 5–6 Å for HQ and AP and 6–8 Å for ODA. These are all reasonable figures considering that the diameter of a benzene ring is about 2.8 Å and ODA is a much bigger molecule than HQ or AP. Interestingly, the density of HQ in the fitted data is much lower than that of AP or ODA, suggesting a less efficient filling in the layer. The roughness parameters for the organic layers might seem rather large considering that the layers are less than 1 nm thick, but the roughness values represent interfacial roughness with ZnO and thus are dominated by the roughness of the much thicker ZnO layers.

The FTIR measurements were performed on hybrid films grown on silicon with a 3:1 ZnO to organic layer ratio in order to see the organic layers more effectively; the spectra

are shown in Fig. 3. There are naturally slight differences between the spectra of the films grown with the different organic constituents, but they all clearly show the presence of a benzene ring as well as C–O bonds, which are common to all the three organic precursors tested here. The largest difference between the spectra is in the intensities of the absorption peaks, with ZnO:HQ giving clearly the strongest peaks and ZnO:AP displaying quite weak peaks. There is also little sign of C–N or Zn–N bond absorptions in the AP and ODA spectra, though this may just be due to the fact that the corresponding absorption peaks would be expected to be very close to those of C–O and Zn–O peaks and thus the peaks could merge. The aforementioned observations, coupled with the lack of any unexpected absorption peaks, confirm that the organic constituents do not break down when reacting with the ZnO surface and precursors, but are incorporated into the films without significant changes in their structure. A rather wide peak attributed to O–H bonds can also be seen in the spectra, which indicates either the presence of small amounts of unreacted –OH groups at the inorganic–organic interfaces or the incorporation of water into the structure possibly from exposure to moisture in air. The samples were, however, measured immediately after removal from the ALD reactor, so there would seem to be little time for significant amounts of water to be able to diffuse into the structure. The –OH group peak could also conceivably result from the intercalation of water into the film structure during H<sub>2</sub>O pulses in the ALD process, but this would also seem to be somewhat unlikely due to the lack of a –OH peak in the FTIR spectra of ZnO films grown under identical process conditions.

## B. Transport properties

The Seebeck coefficient and resistivity values measured at room temperature from the hybrid films deposited on borosilicate glass are presented in Figs. 4 and 5. There is a curious trend observed in both figures in the way the Seebeck coefficient and resistivity values decrease slightly at low

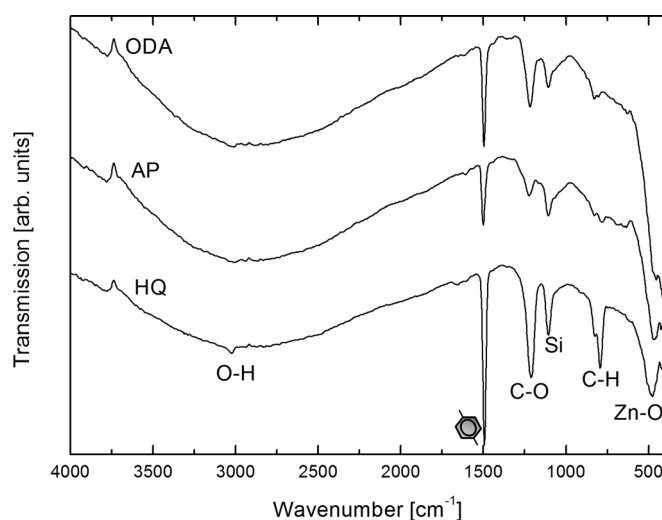


FIG. 3. FTIR spectra for the hybrid films with a 3:1 ZnO to organic (HQ, AP or ODA) layer ratio.

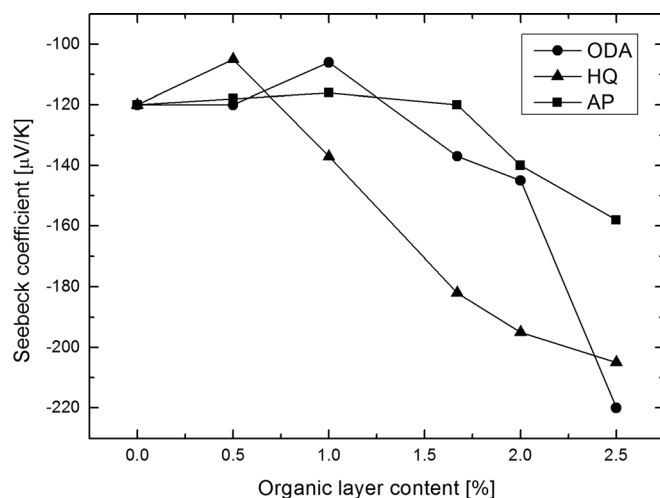


FIG. 4. Room-temperature Seebeck coefficient values for the ZnO:organic hybrid films. Here, the organic layer content is presented as a percentage value of the total number of layers based on the ALD/MLD pulsing sequence, e.g., a ratio of 199:1 becomes 0.5%.

concentrations of organic constituents and then increase as the organic layer content is increased. This corresponds to an increase in carrier concentration followed by a decrease, and there are differences in the magnitude of this effect between the different organic precursors. The ZnO:ODA system shows little effect in its Seebeck coefficient until the ZnO to ODA ratio reaches 99:1, while AP layers have a smaller effect overall. The minimum and maximum values for the Seebeck coefficient within the range of the tested ZnO:organic ratios also vary considerably with the different organic molecules. Resistivity values in principle show a similar trend, although there are some differences compared with the development of the Seebeck coefficient values.

Overall, HQ and ODA have quite similar effects on ZnO's transport properties, but the influence of AP is very small on both Seebeck coefficient and resistivity. This is particularly interesting when one considers that HQ and AP

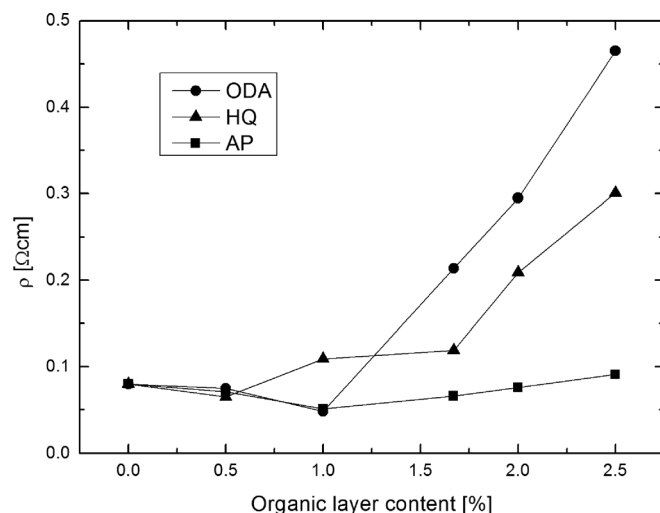


FIG. 5. Room-temperature resistivity values for the ZnO:organic hybrid films. The organic layer content is presented as a percentage of the total number of layers in the pulsing sequence in the same way as in Fig. 4.

have very similar structures, their only difference being in the  $-\text{NH}_2$  group of AP, which replaces one of HQ's  $-\text{OH}$  groups. Even though the FTIR spectra did not show conclusive evidence of the presence of nitrogen bonds in the structure, taking into account the superlattice peak shapes observed in the XRR spectra, it would seem safe to assume that there is a reaction between DEZ and the  $-\text{NH}_2$  groups of AP and ODA that sustains the film growth after the MLD pulses. The nature of the resulting bond, i.e., the bond between the inorganic and organic species going through nitrogen instead of oxygen, can have a large effect on the transport properties of the whole hybrid structure, as evidenced by the differences in the transport properties of the ZnO:AP and ZnO:HQ films. On the other hand, ODA, which can be thought of as two AP molecules joined at the  $-\text{OH}$  group-containing ends and thus would react with DEZ through its  $-\text{NH}_2$  groups, affects ZnO's transport properties in a very similar way to HQ. Based on the current results, though, it is difficult to speculate on the basis of the different behaviors observed with the three organic precursors, so further study will be needed to elucidate the nature of the effect of the bonds between the inorganic and organic species on the transport properties of the hybrid compound as a whole.

#### IV. SUMMARY AND CONCLUSIONS

We have demonstrated the applicability of the ALD/MLD technique in fabricating hybrid inorganic–organic superlattice structures consisting of periodically repeating single layers of organic constituents within a ZnO framework. Three different organic molecules were shown to form superlattices with ZnO as verified by XRR measurements, and FTIR studies confirmed the presence of the unchanged organic precursors in the resultant superlattice films. A non-linear effect on the films' transport properties was observed from the incorporation of the organic layers into ZnO. The magnitude of the effect varied between the different organic constituents, but they all demonstrated a trend consistent with an increase in carrier concentration at low concentrations of organic layers followed by a rather large decrease at higher concentrations.

#### ACKNOWLEDGMENTS

This work was supported by grants from Academy of Finland (Grant No. 255562) and Aalto Energy Efficiency Research Programme.

<sup>1</sup>H. K. Schmidt, *Macromol. Symp.* **101**, 333 (1996).

<sup>2</sup>S.-J. Cho, I.-S. Bae, H.-D. Jeong, and J.-H. Boo, *Appl. Surf. Sci.* **254**, 7817 (2008).

<sup>3</sup>S. Jeong, W.-H. Jang, and J. Moon, *Thin Solid Films* **466**, 204 (2004).

<sup>4</sup>A. A. Dameron, D. Seghete, B. B. Burton, S. D. Davidson, A. S. Cavanagh, J. A. Bertrand, and S. M. George, *Chem. Mater.* **20**, 3315 (2008).

<sup>5</sup>S. M. George, B. Yoon, and A. A. Dameron, *Acc. Chem. Res.* **42**, 498 (2009).

<sup>6</sup>S. George, A. Dameron, Y. Du, N. M. Adamczyk, and S. Davidson, *ECS Trans.* **11**, 81 (2007).

- <sup>7</sup>B. H. Lee, M. K. Ryu, S.-Y. Choi, K.-H. Lee, S. Im, and M. M. Sung, *J. Am. Chem. Soc.* **129**, 16034 (2007).
- <sup>8</sup>B. Yoon, D. Seghete, A. S. Cavanagh, and S. M. George, *Chem. Mater.* **21**, 5365 (2009).
- <sup>9</sup>Q. Peng, B. Gong, R. M. VanGundy, and G. N. Parsons, *Chem. Mater.* **21**, 820 (2009).
- <sup>10</sup>B. Yoon, J. L. O’Patchen, D. Seghete, A. S. Cavanagh, and S. M. George, *Chem. Vap. Deposition* **15**, 112 (2009).
- <sup>11</sup>A. Sood, P. Sundberg, J. Malm, and M. Karppinen, *Appl. Surf. Sci.* **257**, 6435 (2011).
- <sup>12</sup>B. H. Lee, B. Yoon, V. R. Anderson, and S. M. George, *J. Phys. Chem. C* **116**, 3250 (2012).
- <sup>13</sup>L. Ghazaryan, E.-B. Kley, A. Tünnermann, and A. V. Szeghalmi, *J. Vac. Sci. Technol. A* **31**, 01A149 (2013).
- <sup>14</sup>P. Sundberg, A. Sood, X. Liu, L.-S. Johansson, and M. Karppinen, *Dalton Trans.* **41**, 10731 (2012).
- <sup>15</sup>A. I. Abdulagatov, R. A. Hall, J. L. Sutherland, B. H. Lee, A. S. Cavanagh, and S. M. George, *Chem. Mater.* **24**, 2854 (2012).
- <sup>16</sup>A. Sood, P. Sundberg, and M. Karppinen, *Dalton Trans.* **42**, 3869 (2013).
- <sup>17</sup>K.-H. Yoon, K.-S. Han, and M.-M. Sung, *Nanoscale Res. Lett.* **7**, 71 (2012).
- <sup>18</sup>R. Triboulet and J. Perrière, *Prog. Cryst. Growth Charact. Mater.* **47**, 65 (2003).
- <sup>19</sup>G. Luka, M. Godlewski, E. Guziewicz, P. Stakhira, V. Cherpak, and D. Vlynyuk, *Semicond. Sci. Technol.* **27**, 074006 (2012).
- <sup>20</sup>B. Yoon, B. H. Lee, and S. M. George, *J. Phys. Chem. C* **116**, 24784 (2012).
- <sup>21</sup>J. O. Sofo and G. D. Mahan, *Appl. Phys. Lett.* **65**, 2690 (1994).
- <sup>22</sup>R. Venkatasubramanian, E. Siivola, T. Colpitts, and B. O’Quinn, *Nature* **413**, 597 (2001).
- <sup>23</sup>J. Carrete, N. Mingo, G. Tian, H. Ågren, A. Baev, and P. N. Prasad, *J. Phys. Chem. C* **116**, 10881 (2012).